Hot Topics in Thermal Analysis and Calorimetry

VOLUME 8

Series Editor
Judit Simon, *Budapest University of Technology and Economics, Hungary*

Jaroslav Šesták • Jiří J. Mareš • Pavel Hubík
Editors

Glassy, Amorphous and Nano-Crystalline Materials

Thermal Physics, Analysis, Structure and Properties

Springer

Editors
Jaroslav Šesták
New Technologies –
Research Centre in the Westbohemian
Region
University of West Bohemia
Univerzitní 8
30614 Plzeň
Czech Republic
sestak@fzu.cz

Pavel Hubík
Institute of Physics, v.v.i.
Academy of Sciences
of the Czech Republic
Cukrovarnická 10
16200 Prague 6
Czech Republic
hubik@fzu.cz

Jiří J. Mareš
Institute of Physics, v.v.i.
Academy of Sciences
of the Czech Republic
Cukrovarnická 10
16200 Prague 6
Czech Republic
maresjj@fzu.cz

ISBN 978-90-481-2881-5 e-ISBN 978-90-481-2882-2
DOI 10.1007/978-90-481-2882-2
Springer Dordrecht London Heidelberg New York

Library of Congress Control Number: 2010938473

Preface

Early Research into Amorphous Semiconductors

Numerous aspects of physics and chemistry of non-crystalline solids and glassy state which are discussed in the present book can only hardly be prefaced without rude simplification. Therefore, let us make instead a short excursion to the prehistory of research into amorphous semiconductors, the topic on which the common epistemological features of the other subjects treated in this book may be demonstrated.

It is a matter of fact that in everyday life we encounter more frequently non-crystalline than crystalline solids. We can even with some exaggeration say that in the Nature the perfect crystals are as rare as diamonds. In spite of that, the existence of the class of non-crystalline materials has been recognized only recently. One of the reasons for such a state of the art is probably the fact that the positivistic continuous model of matter dominated till the end of the nineteenth century and that the fundamental conjectures of atomism were too closely bound up with the idea of the regular ordering of atoms; early atomic theories accounting for the regular shape of snow flakes [1] and for the anisotropy of optical properties of transparent crystals [2], namely, exploited the idea that such a regularity is due to the closest filling of the space by identical hard polyhedrons or spheres, atoms. Denying atomic order in solids would thus undermine the strongest intuitive argument in favour of atomism, namely, that just the satisfaction of geometrical constrains between neighbouring atoms and their close packing accounts for actually observed regular shape of crystals. Interestingly enough, in the scientific disputations about the structure of matter, the existence of glass, for a long time known amorphous, i.e. "shapeless" material par excellence, was tacitly ignored.

The serious attempts to treat the atomic structure of amorphous or glassy state are thus relatively recent, belonging to the first half of the twentieth century. The glass was at that time considered to be nothing but undercooled liquid i.e. a solid having essentially the atomic structure of original melt. Such a picture was an immediate consequence of phenomenological principle of continuity between

Chapter 16

Emanation Thermal Analysis as a Method for Diffusion Structural Diagnostics of Zircon and Brannerite Minerals

Vladimír Balek, Iraida M. Bountseva, and Igor von Beckman

16.1 Emanation Thermal Analysis of Solids

Emanation thermal analysis (ETA) [1–3] based on the measurement of the radon release from samples, is one of the methods used in the diffusion structure diagnostics of solids. Changes in surface morphology and microstructure of solids during their thermal treatments and changes due to chemical, mechanical or radiation interactions can be studied by the emanation thermal analysis method.

As most of the solids to be investigated do not naturally contain atoms of radon it is necessary to introduce the radon atoms in the samples prior to the ETA measurements.

To introduce the radioactive trace ^{220}Rn into solids, the samples are labelled by parent radio-nuclides ^{228}Th and ^{224}Ra, serving as a quasi-permanent source of radon atoms ^{220}Rn. The used specific activity of the parent radionuclide ^{228}Th is in the order 10^5 Bq g^{-1} of the sample.

16.1.1 Radon Atoms Implantation into Solids by the Recoil Energy of α-Decay

Atoms of the ^{220}Rn radon radionuclide are formed by a spontaneous α-decay of ^{228}Th and ^{224}Ra radio-nuclides according to scheme Eq. 16.1

V. Balek (✉)
Nuclear Research Institute Řež, plc, 250 68 Řež, Czech Republic
e-mail: bal@ujv.cz

I.M. Bountseva and I. von Beckman
Faculty of Chemistry
Moscow MV Lomonosov State University, Moscow 199234, Russia

J. Šesták et al. (eds.), *Glassy, Amorphous and Nano-Crystalline Materials*,
Hot Topics in Thermal Analysis and Calorimetry 8, DOI 10.1007/978-90-481-2882-2_16,

$$^{228}\mathrm{Th} \xrightarrow[T_{1/2}=1.9\mathrm{y}]{\alpha} {}^{224}\mathrm{Ra} \xrightarrow[T_{1/2}=3.8\mathrm{y}]{\alpha} {}^{220}\mathrm{Rn} \xrightarrow[T_{1/2}=55\mathrm{s}]{\alpha} \qquad (16.1)$$

and the ^{220}Rn atoms can be introduced into the solid owing to the recoil energy of the spontaneous α-decay (85 keV/atom). The samples can be labelled by using an adsorption of traces of ^{228}Th as nitrate from a solution.

Due to the energy of the spontaneous α-decay of ^{228}Th and ^{224}Ra radio-nuclides the atoms of ^{220}Rn can penetrate into the sample several tens of nanometres from the surface depending on the composition of the materials.The values of the maximum penetration depths of ^{220}Rn were determined by the Monte Carlo method using TRIM code [4], e.g. for SiO_2: 65.4 nm, for zircon ($ZrSiO_4$): 60 nm and brannerite mineral ($U_{1-x}Ti_{2+x}O_6$): 60 nm.

Radon atoms can be trapped in solids at structure defects such as vacancy clusters, grain boundaries and pores. The structure defects in the solids can serve both as traps and as diffusion paths for radon atoms.

16.1.2 Mechanisms of the Radon Release from Solids

The radon formed by the spontaneous α-decay of ^{224}Ra may escape from the solid either by recoil energy ejection or by diffusion. The term emanation rate, E, has been used to express the release of radon from solids. It is defined as the ratio of the radon release rate to the rate of radon formation by the spontaneous α-decay of ^{228}Th and ^{224}Ra in the investigated solids.

It has been determined experimentally (in relative units) as $E = A_\alpha/A_{\mathrm{total}}$, where A_α is the α-radioactivity of radon released in unit time from the labelled sample and A_{total} is the total γ -radioactivity of the labelled sample. The A_{total} value is proportional to the rate of radon formation in the sample.

In the evaluation of the radon release from solids several mechanisms have been supposed, namely the radon release by recoil mechanism, the diffusion in open pores, and the volume diffusion mechanism.

The experimentally obtained values of the emanation rate, E, can be considered as:

$$\mathrm{E} = \mathrm{E(recoil)} + \mathrm{E(pores)} + \mathrm{E(solid)} \qquad (16.2)$$

The emanation rate due to recoil, E (recoil), can be expressed as

$$\mathrm{E(recoil)} = \mathrm{K_1 S_1} \qquad (16.3)$$

where K_1 is a temperature independent constant, proportional to the penetration depth of recoiled radon atoms in solids investigated and S_1 is external surface area of sample particles. The path of recoiled atoms of radon is dependent on the "nuclear stopping power" of the sample material.

The emanation rate due to diffusion in pores, E (pores), is expressed as

$$E(\text{pores}) = K_2 S_2 \tag{16.4}$$

where K_2 is a constant that depends on temperature and S_2 is internal surface area of the sample depending on the surface of open pores, cracks and intergranular space.

The emanation rate due to volume diffusion mechanism, E (solid), is expressed as

$$E(\text{solid}) = K_3 \exp(-Q/2\mathbf{R}T) S_3 \tag{16.5}$$

where K_3 is a constant related to the atomic properties of the lattice, Q is the activation energy of Rn diffusion in the solid, S_3 is surface area, **R** is molar gas constant, and T is temperature.

The growth of the emanation rate values, E (T), may characterize an increase of the surface area of interfaces, whereas a decrease in the E(T) may reflect processes like closing up structure irregularities that serve as paths for the radon migration, closing pores and/or a decrease in the surface area of the interfaces [3–6].

16.2 Application of the Emanation Thermal Analysis in the Diffusion Structural Diagnostics of Solids

The equipment for the emanation thermal analysis (ETA) was developed in the 1960s [1, 2]. Since that time the ETA method was used in various investigations, e.g. the re-crystallization of solids, annealing of structure defects and changes in the defect state of both crystalline and amorphous solids, sintering, phase changes, the characterization of surface and morphology changes accompanying chemical reactions in solids and on their surfaces, including the thermal degradation, solid–gas, solid–liquid, and solid–solid interactions [7–11]. The ETA made it possible to reveal even fine changes in poorly crystalline or amorphous solids. Differences in the morphology and behaviour of samples prepared by the sol–gel technique under different conditions were revealed by the ETA.

Changes in defects annealing and pore sintering of the samples were characterized by using the ETA results under in situ conditions of their heat treatments. The determination of optimized conditions for the preparation and thermal treatments of advanced ceramic materials was achieved [10, 11]. By this way the ETA results contributed to the solution of practical tasks in the materials technology.

Recently, this method made it possible to characterize the thermal stability of ceramic materials designed for the immobilization/encapsulation of high level radioactive waste [12]. Moreover, the thermal stability of self- irradiated amorphous minerals that serve as natural analogues of the ceramic matrices was evaluated by using the emanation thermal analysis.

In the study of the self- irradiated metamict materials the ETA measurements were carried out by using modified NETZSCH DTA-ETA equipment, Type 404. Details of the measurements and the data treatments are described elsewhere [2–6]. During the ETA measurements the samples were heated at the rate of 6 K min^{-1} in air (zircon sample) and argon (brannerite sample). The specific activity of the labelled samples was 10^5 Bq g^{-1}.The used amounts of the samples were 0.02 and 0.1 g respectively. During the ETA measurements, a constant flow of the carrier gas (air, nitrogen, or another gas) has been used to take the radionuclide of radon of ^{220}Rn released by the sample into the detector of α-activity of radon (semiconductor detectors).

16.2.1 Thermal Behaviour of Natural Zircon Mineral

Natural zircon mineral (general formula $ZrSiO_4$), containing an average concentration up to 0.4% of uranium and 0.2% of thorium, has attracted much interest from both fundamental and technological view points. The α-particles and heavy recoil nuclei released during the decay of radioactive impurities (typically ^{238}U, ^{235}U and ^{232}Th) interact with the surrounding crystalline matrix displacing atoms from their equilibrium positions [13]. Over geological periods of time this process disrupts the crystalline order to such a point that specimens covering all the stages from fully crystalline to amorphous can be found, depending on the uranium/thorium content.

Understanding the radiation effects in crystalline zircon and the determination of the structure of the aperiodic state are essential to ensure the reliability of zircon based ceramics for nuclear waste disposition [13, 14]. During nuclear disintegration, the emission of the α-particle is accompanied by a recoil nucleus. Amorphization taking place in natural zircon is called metamictization. The α-particles have energy of 4–6 MeV, and almost all the energy is dissipated by the ionization processes. It is believed that various isolated defects, such as Frenkel pairs, are formed along their paths. A number of studies have been devoted to structural changes of zircon under irradiation, in particular to understanding the amorphization and/or metamictization process [15]. This process can lead to an increased solubility and fracturing [16].

Ceramic forms used in the encapsulation of nuclear waste are subjected to a similar transformation, with the corresponding variation of their physical and chemical properties. An understanding of radiation effects in crystalline zircon and a determination of the structure of the aperiodic state are essential to ensure the reliability of zircon and related ceramics for nuclear waste disposition [13, 14].

Zircon ceramics can incorporate significant amount of UO_2, PuO_2 or ThO_2 in a solid solution with ZrO_2. The zircon undergoes an amorphization promoted by α-decay events of radiogenic elements. During the nuclear disintegration, the emission of an α-particle is accompanied by a recoil nucleus and ballistic collisions of the recoil nucleus cause displacement cascades. A number of studies have been

devoted to the evolution of amorphous zircon under irradiation, in particular to understanding of the metamictization process [15].

Natural zircon mineral sample characterized by ETA was from the locality Sri Lanka. The sample was X-ray amorphous [16].

Figure 16.1 shows ETA results of the zircon mineral sample measured on heating (curve 1a) in air flow in the temperature range 20–1,100°C and subsequent cooling (curve 1b). The increase of the emanation rate, E, observed in the temperature range of 170–250°C characterized the diffusion mobility of radon atoms along surface cracks and other subsurface defects, the subsequent decrease of the E values in the range 250–420°C can be ascribed to healing the surface and subsurface defects.

We supposed that the increase of the emanation rate, E, in the range 420–750°C is due to the radon diffusion along structure irregularities in the amorphous zircon. The phase transformation of initially amorphous zircon was characterized by the decrease of the emanation rate values E in the range 750–950°C. From ETA results of the amorphous zircon mineral sample measured on heating to 1,200°C and subsequent cooling to room temperature it followed that the microstructure changes taking place in the sample on heating were irreversible.

The results of DSC measured on a parallel sample of amorphous/metamict zircon are demonstrated in Fig. 16.1 as the full line curve. The transformation of amorphous zircon to the crystalline zircon was characterized by a DSC exothermal effect with the maximum at 918°C.

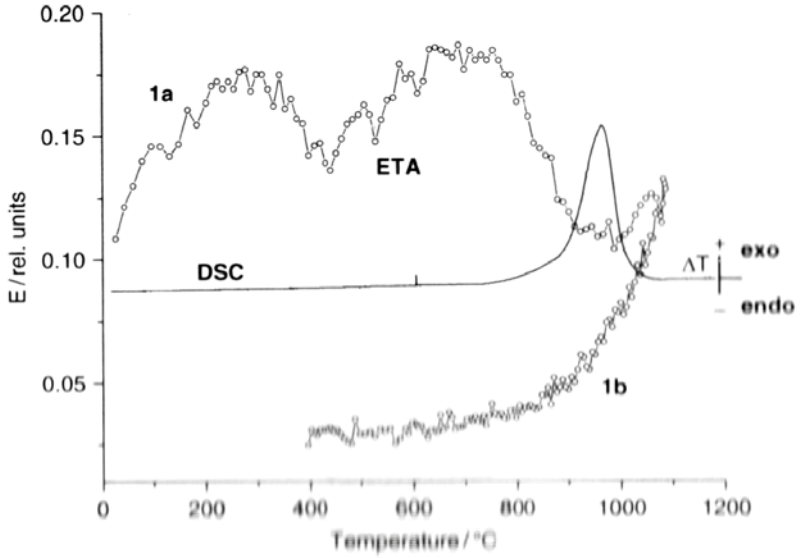

Fig. 16.1 ETA results (points) of natural zircon mineral sample measured on heating (curve 1a) and subsequent cooling (curve 1b) in air in the range 20–1,100°C. The DSC results measured on the sample heating are depicted as the *full line curve*

16.2.2 Thermal Behaviour of Natural Brannerite Mineral

Brannerite mineral (general formula $U_{1-x}Ti_{2+x}O_6$) has been found in nature as amorphous due to α-decay damage caused by high content of U, Th. The formula of natural brannerite can also be written $(U, Th)_{1-x}Ti_{2+x}O_6$. The natural brannerite generally contains impurity elements like Pb, Ca, Th, Y and rare earth elements (REE) on the U-site and Si, Al and Fe on the Ti-site. The brannerite is a minor phase in titanate-based ceramics designed for the geological immobilization of surplus Pu [17, 18]. Therefore, it was of interest to investigate the thermal behaviour of the metamict brannerite mineral as a natural analogue of the brannerite ceramics to be used for immobilization of hazardous radioactive elements.

The diffusion structural diagnostics based on the results of emanation thermal analysis (ETA) made it possible to characterize the annealing of the structure irregularities in the brannerite mineral sample on heating to various temperatures up to 1,200°C. Natural brannerite mineral was from the locality El Cabril mine near Cordoba, Spain. The sample was X-ray amorphous and contained Ca, Pb and other impurity elements [17].

Figure 16.2 shows the ETA results of the metamict brannerite mineral measured during heating in argon in the range 20–1,200°C and subsequent cooling. The increase of emanation rate, E, observed on the sample heating in the range of 40–300°C characterized the diffusion mobility of radon atoms along surface cracks and other subsurface defects to depth of 60 nm.

The slight decrease of $E(T)$ observed in the temperature range of 400–500°C (curve 1a, Fig. 16.2) was ascribed to healing surface cracks and voids. The decrease

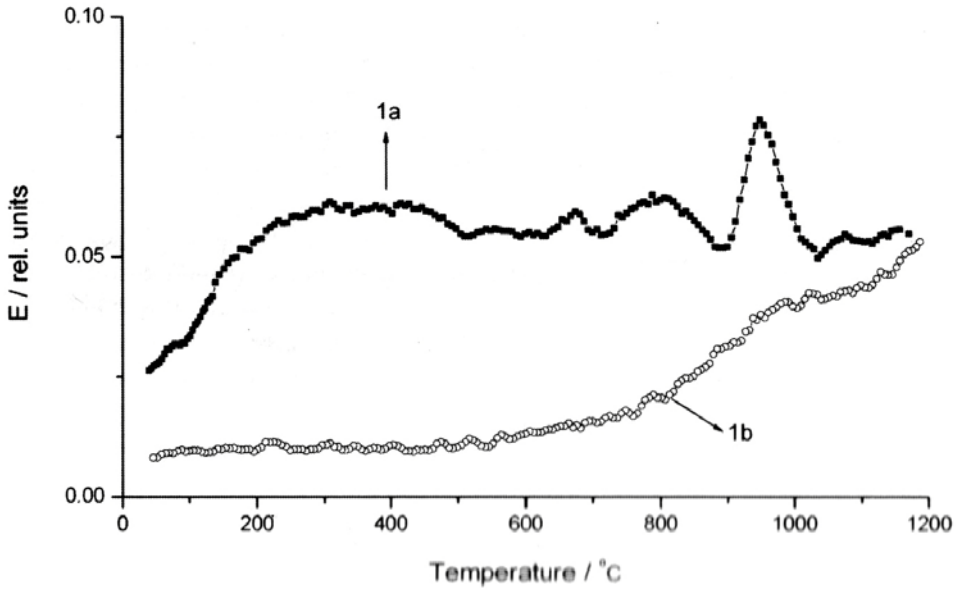

Fig. 16.2 ETA results of natural brannerite mineral sample measured on heating (curve 1a) and subsequent cooling (1b) in argon in the range 2–1,200°C

of the emanation rate *E(T)* observed on the ETA curve in the range 800–880°C, corresponding to the healing microstructure irregularities, was considered as a first step of the formation of crystalline brannerite. The increase of *E(T)* observed in range 900–965°C followed by the sharp decrease of *E(T)* in the range 970–1,020°C indicated the formation of the crystalline brannerite phase, as confirmed by XRD spectroscopy [17, 19]. From ETA results of the brannerite mineral sample measured on heating up to 1,200°C and subsequent cooling it followed that the microstructure changes on sample heating are irreversible.

The release of CO_2 was detected by mass spectrometry of evolved gases in the temperature range 700–800°C [17] due to the thermal degradation of minor carbonate containing components of the sample. The release of CO_2 gave rise to the sample porosity [17]. It was of interest to investigate the self-irradiated metamict brannerite mineral during "step by step" heating and subsequent cooling of the sample to the temperatures of 300, 550, 750, 880, 1,020 and 1,150°C, respectively. Results of ETA measured by the "step by step" heating runs (Fig. 16.3) made it possible to compare the annealing of microstructure irregularities of the sample in the selected temperature intervals.

As it follows from the ETA results in Fig. 16.3, the "step by step" heating of the sample to these temperatures caused a decrease of the amount of structure irregularities serving as radon diffusion paths.

A good reproducibility of the ETA results measured on heating from 20°C to 300°C is obvious from the comparison of the results in Fig. 16.3, curves 2a and 1a.

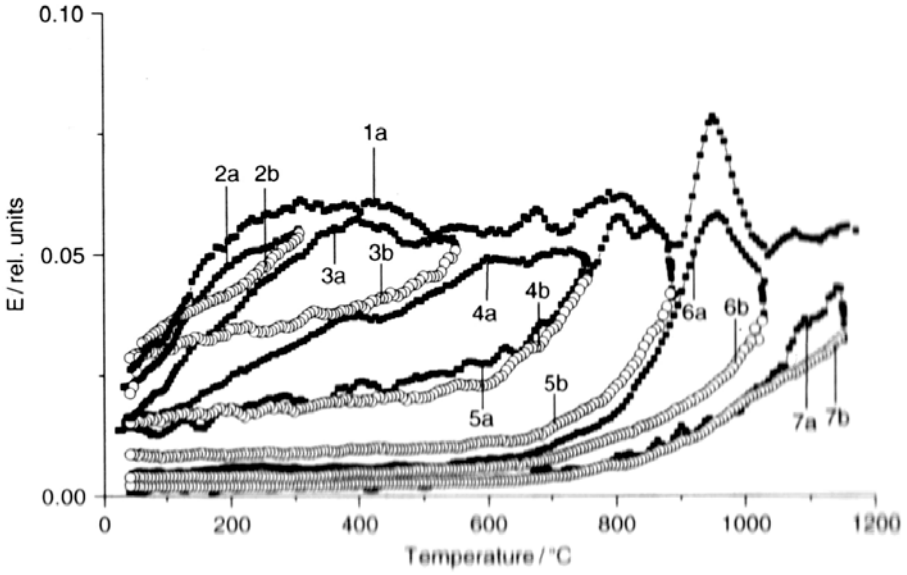

Fig. 16.3 ETA results of natural brannerite mineral sample measured on heating and subsequent cooling in argon in the range 20–1,150°C; curve 1a corresponds to the "as received" sample measured during heating from 20°C to 1,150°C, curves 2a/2b, 3a/3b, 4a/4b, 5a/5b, 6a/6b and 7a/7b were measured with a parallel samples pre-heated to the temperatures of 300, 550, 750, 880 and 1,020°C, respectively

The ETA curves 3a/3b, 4a/4b and 5a/5b characterized the thermal behaviour of the metamict brannerite sample pre-heated to 300 and 750°C, respectively. The increase of the emanation rate, E, in the temperature range of 20–360°C, due to the diffusion of radon along micropores in the sample, was followed by the decrease of E, characterizing the partial healing of voids and structure irregularities that served as diffusion pathways for radon.

The ETA curves 6a/6b in Fig. 16.3 characterized the thermal behaviour of the sample pre-heated to 880°C. As already observed by curve 1a the amount of structure irregularities serving as radon diffusion paths further diminished in the sample pre-heated to 880°C. The decrease of the emanation rate on sample observed on heating in the range of 970–1,020°C indicated the next step of the formation of crystalline brannerite. A good reproducibility of the ETA measurements can be seen from the temperature coincidence of the effects on the curve 1a and curve 6a in Fig. 16.3.

From curves 7a/7b characterizing the thermal behaviour of the sample pre-heated to 1,020°C, it is obvious that after the pre-heating the sample to this temperature an irreversible crystallization of amorphous self-irradiated brannerite mineral took place.

From Fig. 16.3 it is obvious that the amount of structure irregularities serving as radon diffusion paths further diminished and the radon permeability in the pre-heated brannerite samples decreased with the temperature used for pre-heating of the samples.

Values of the emanation rate, E_{RT}, measured at room temperature before and after each heating run were used for the assessment of the relative changes of the surface area affected by the heat treatments used. The E_{RT} values summarized in Table 16.1 are in agreement with our considerations of the annealing of surface area and subsurface irregularities.

From the temperature dependences of the emanation rate, $E(T)$, measured during heating to selected temperatures and subsequent cooling, the decrease in the amount of radon diffusion paths was assessed. To this aim we used the parameter ξ defined in Eq. 16.6 as:

Table 16.1 Microstructure defects characteristics of natural self-irradiated brannerite mineral sample pre-heated to various temperatures

ETA curves measured on heating/cooling	Temperature of sample pre-heating	Defect amount characteristics ξ^*	E_{RT} [rel. units]	$\Delta\xi^{**}$ [%]
Curves 1a/1b, Fig. 16.2	As received	38.1	0.026	100
Curves 2a/2b, Fig. 16.3	As received	0.41	0.023	1.08
Curves 3a/3b, Fig. 16.3	300°C	3.82	0.017	10.02
Curves 4a/4b, Fig. 16.3	550°C	10.26	0.015	26.93
Curves 5a/5b, Fig. 16.3	750°C	13.62	0.014	35.75
Curves 6a/6b, Fig. 16.3	880°C	6.30	0.005	16.54
Curves 7a/7b, Fig. 16.3	1,020°C	0.98	0.001	2.57

* $\xi(T_{\max}) = \int_{T_{\min}}^{T_{\max}} E(T)_{heating}dT - \int_{T_{\min}}^{T_{\max}} E(T)_{cooling}dT$ ** $\Delta\xi = \frac{\xi_2}{\xi_1} \times 100\,[\%]$

$$\xi(T_{max}) = \int_{T_{min}}^{T_{max}} E(T)_{heating}dT - \int_{T_{min}}^{T_{max}} E(T)_{cooling}dT \qquad (16.6)$$

Moreover, values of $\Delta\xi$ (see Eq. 16.7) were calculated with the aim to compare the amounts of the annealed microstructure defects during the "step by step" heating of the sample. The difference of integrals used for the assessment of the amount of the microstructure defects can be expressed as $\Delta\xi$ defined as

$$\Delta\xi = \frac{\xi_n}{\xi_1} \times 100[\%] \qquad (16.7)$$

As it followed from values of ξ and $\Delta\xi$ summarized in Table 16.1, the most significant decrease of the structure irregularities serving as diffusion paths for radon diffusion was annealed prior to the crystallization of the sample in the range of 970–1,020°C.

Figure 16.4 depicts a comparison of the relative amount of structure irregularities, expressed by parameter ξ, that were annealed during heat treatments to the selected temperatures.

It was shown that the emanation thermal analysis revealed differences in the amount of structure irregularities that served as radon diffusion paths in the brannerite

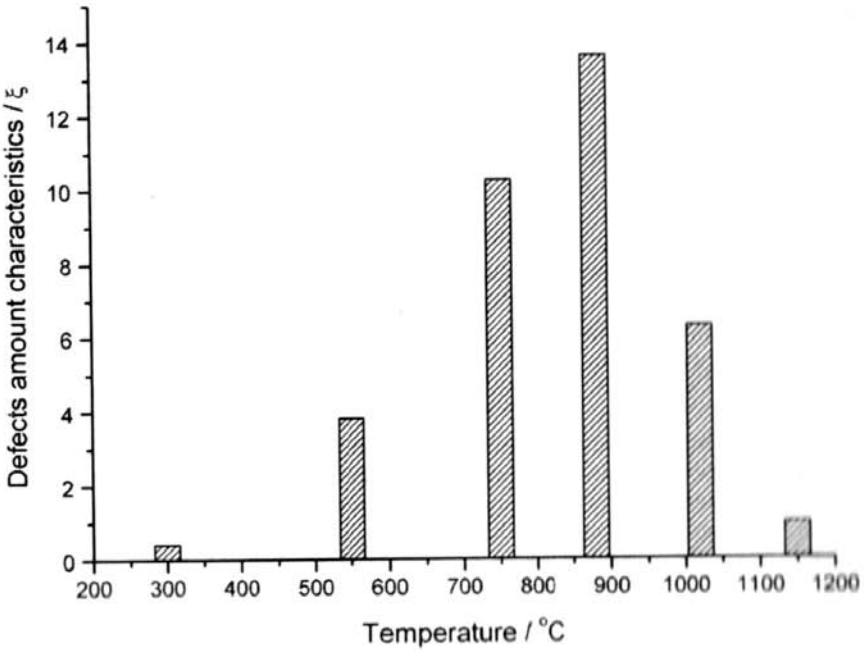

Fig. 16.4 Relative amounts of micro structure irregularities in natural brannerite sample healed in the heating runs to temperatures 20–300, 20–550, 20–750, 20–880, 20–1,020 and 20–1,150°C. Parameter ξ was used to characterize the amount of structure irregularities of the following samples: preheated to 300, 550, 750, 880 and 1,020°C respectively

samples. Additional information about thermal behaviour of self-irradiated metamict minerals was obtained by using the diffusion structural diagnostics.

Acknowledgments Authors thank to the Ministry of Education, Youth and Sports of the Czech Republic for the support (Project MSM 2672244501).

References

1. Balek V (1978) Emanation thermal analysis. Thermochim Acta 22:1–156
2. Balek V (1991) Emanation thermal analysis and its application potential. Thermochim Acta 192:1–17
3. Balek V, Šubrt J, Mitsuhashi T, Beckman IN, Györyová K (2002) Emanation thermal analysis: ready to fulfil the future needs of materials characterization. J Therm Anal Calorim 67:15–35
4. Ziegler JF, Biersack JP, Littmark U (1985) The stopping and range of ions in solids. Pergamon, New York
5. Beckman IN, Balek V (2002) Theory of emanation thermal analysis XI. Radon diffusion as the probe of microstructure changes in solids. J Therm Anal Calorim 67:49–61
6. Emmerich WD, Balek V (1973) Simultaneous application of DTA, TG, DTG, and emanation thermal analysis. High Temp-High Press 5:67
7. Balek V, Tölgyessy J (1984) Emanation thermal analysis and other radiometric emanation methods. In: Svehla G (ed) Wilson and Wilson's comprehensive analytical chemistry, Part XIIC. Elsevier Science, Amsterdam
8. Balek V, Brown ME (1998) Less common techniques. In: Brown ME (ed) Handbook on thermal analysis and calorimetry, vol 1. Elsevier Science BV, Amsterdam, pp 445–471
9. Balek V (1989) Characterization of high-tech materials by means of emanation thermal analysis. J Therm Anal 35:405–427
10. Balek V, Šesták J (1988) Use of emanation thermal analysis in characterization of superconducting $YBa_2Cu_3O_x$. Thermochim Acta 133:23–26
11. Balek V, Pérez-Rodriguez JL, Pérez-Maqueda LA, Šubrt J, Poyato J (2007) Thermal behaviour of ground vermiculite. J Therm Anal Calorim 88:819–823
12. Balek V, Zhang Y, Zeleňák V, Šubrt J, Beckman IN (2008) Emanation thermal analysis study of brannerite ceramics for immobilization of hazardous waste. J Therm Anal Calorim 92:155–160
13. Ríos S, Boffa-Ballaran T (2003) Microstructure of radiation-damage zircon under pressure. J Appl Crystallogr 36:1006–1012
14. Devanathan R, Corrales LR, Weber WJ (2004) Molecular dynamics simulation of disordered zircon. Phys Rev B 69:064115(9)
15. Carrez P, Forterre Ch, Braga D, Leroux H (2003) Phase separation in metamict zircon under electron irradiation. Nucl Instrum Methods B 211:549–555
16. Wang LM, Ewing RC (1992) Detailed in situ study of ion beam-induced amorphization of zircon. Nucl Instrum Methods B 65:324–329
17. Balek V, Vance ER, Zeleňák V, Málek Z, Šubrt J (2007) Use of emanation thermal analysis to characterize thermal reactivity of brannerite mineral. J Therm Anal Calorim 88:93–98
18. Lian J, Wang LM, Lumpkin GR, Ewing RC (2002) Heavy ion irradiation effects of brannerite-type ceramics. Nucl Instrum Methods B 191:565–570
19. Zhang Y, Lumpkin GR, Li H, Blackford MG, Colella M, Carter ML, Vance ER (2006) Recrystallisation of amorphous natural brannerite through annealing: The effect of radiation damage on the chemical durability of brannerite. J Nucl Mater 350:293–300